# HOMOGENEOUS AND HETEROGENEOUS PHOTOREACTIONS OF DECOMPOSITION AND OXIDATION OF CARBOXYLIC ACIDS

M. BIDEAU, B. CLAUDEL†, L. FAURE and M. RACHIMOELLAH‡

*Laboratoire de Cinétique et Génie Chimiques, 404, Institut National des Sciences Appliquées, 20 avenue Albert Einstein, F-69621 Villeurbanne (France)*

(Received December 31, 1986)

## Summary

Decarboxylation and oxidation reactions of carboxylic acids in the presence of various light receivers are reviewed from the experimental and mechanistic standpoints. The homogeneous photoreceivers studied are the ions $UO_2^{2+}$, $Fe^{2+}$ and $Cu^{2+}$. They differ in activity and in selectivity as far as the nature of the hydrocarbons formed by decarboxylation is concerned. The activity of the heterogeneous photocatalyst $TiO_2$ (anatase) in oxidation is shown to be greatly increased in the presence of dissolved substances, *e.g.* $Fe^{3+}$ and $Cu^{2+}$.

## 1. Introduction

The photoreactions of carboxylic acids have long been studied, as reported in a classical textbook [1]. The following primary photochemical steps have been put forward:

$$RCO_2H \rightarrow \begin{cases} R^{\cdot} + CO_2 + H^{\cdot} \\ R^{\cdot} + CO + OH^{\cdot} \\ RH + CO_2 \end{cases}$$

It is worth noting that, at least for the first members of the homologous series, these steps require an irradiation below 240 nm and therefore are of limited practical interest.

Another process which involves carboxylate ions is their oxidative cleavage at the anode of an electrolysis cell (the Kolbe reaction). The following pathways are involved [2]:

†Author to whom correspondence should be addressed.

‡On leave from the Department of Chemical Engineering, Surabaya Institute of Technology, Surabaya, Indonesia.

0047-2670/87/$3.50 

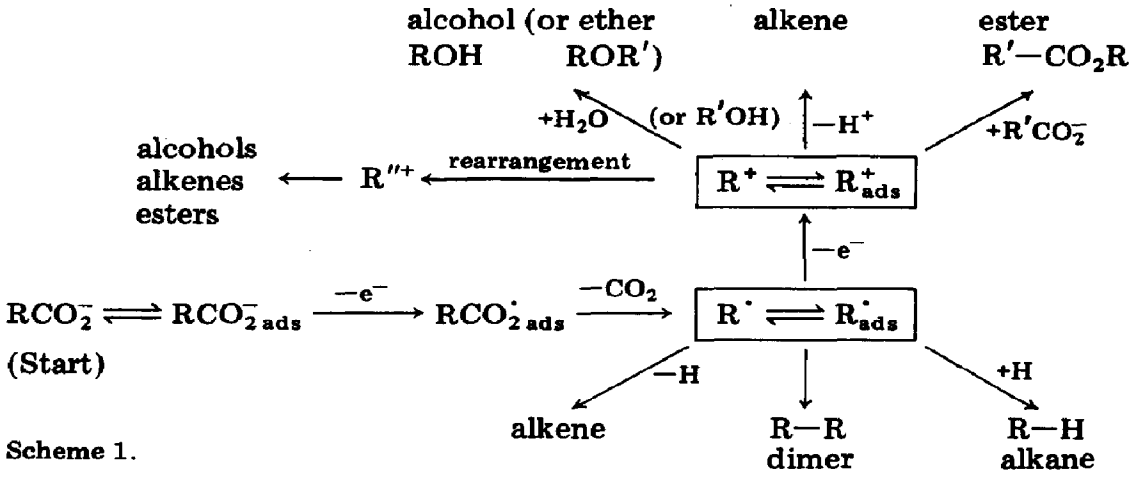


Scheme 1.

Such a scheme is important for our purpose, not because we expect to find all the products of the electrochemical process also in the photochemical reaction, but because it shows which steps are possible in the conversion of carboxylate ion when a convenient electron acceptor exists in the medium.

In this paper we shall discuss the results of these conversions, either in the absence or in the presence of oxygen, and in both cases with a "photoreceiver", the role of which will be stated more precisely. Suffice it to say, for the time being, that it must pick up, directly or indirectly, the luminous emission of a convenient wavelength.

## 2. Experimental devices

Very few experiments have been carried out with gaseous reactants [3]. Most have been realized with aqueous solutions of carboxylic acids. Usually, the gaseous products are removed from the reactor using an inert carrier gas (Fig. 1). Gaseous oxygen is introduced when oxidation is studied. The reaction is followed by an analysis of the solution or of the gaseous effluents or

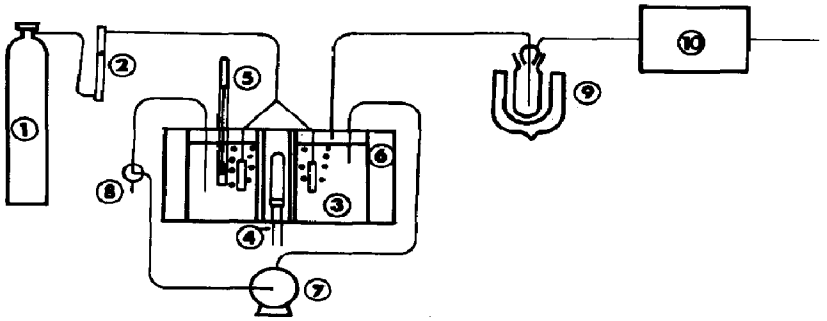


Fig. 1. Schematic diagram of the set-up used for "anaerobic" photocatalysis of carboxylic acids: 1, gas tank (hydrogen or helium); 2, flowmeter; 3, photoreactor; 4, mercury vapour lamp; 5, thermometer; 6, water jacket; 7, recycling pump; 8, sampling valve; 9, cooled trap; 10, gas chromatograph.

of both. A mass balance is, as usual, a prerequisite in any kinetic study, and therefore should be checked whenever possible. From the standpoint of reactor design, the sketched device is a semibatch reactor (a reactor in which one of the reactants is put into it at the beginning, while the other components are either fed or removed). Figures 2 - 5 show how the general scheme can be applied to particular designs called mounts A, B, C and D.

Such reactors are places of interfacial transfers, the importance of which has been pointed out in an earlier publication [4]. In the simple case of a reaction

$$A_l \longrightarrow D_g + E_g$$

which is assumed to occur mainly in the liquid bulk, the mass balance equations read as follows. For A

$$-r_v V_l = \frac{dn_A}{dt}$$

For D in the liquid

$$r_v = k_l a(C_{Dl} - C_{Dl}) + \frac{dC_{Dl}}{dt}$$

For D in the gas

$$k_l a(C_{Dl} - C_{Dl}) V_l = \bar{n}_{D\,out}$$

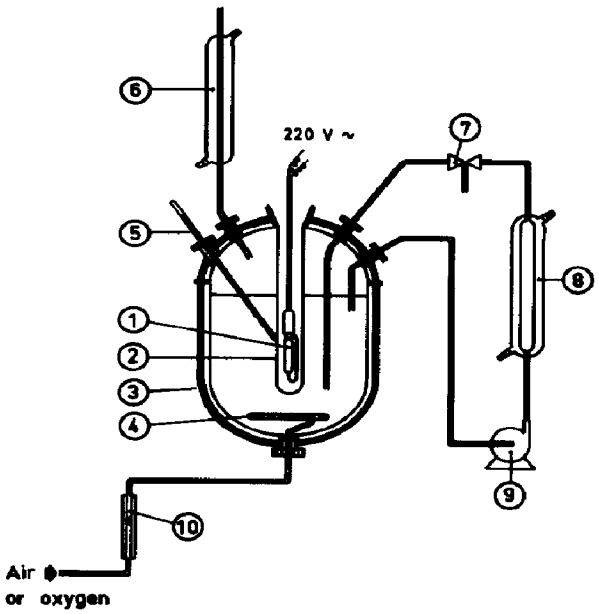


Fig. 2. Photoreactor with immersed lamp (mount A): 1, mercury vapour lamp; 2, Pyrex glass well; 3, reflector; 4, gas disperser; 5, thermometer; 6, cooler; 7, sampling valve; 8, cooler; 9, recycling pump; 10, flowmeter.

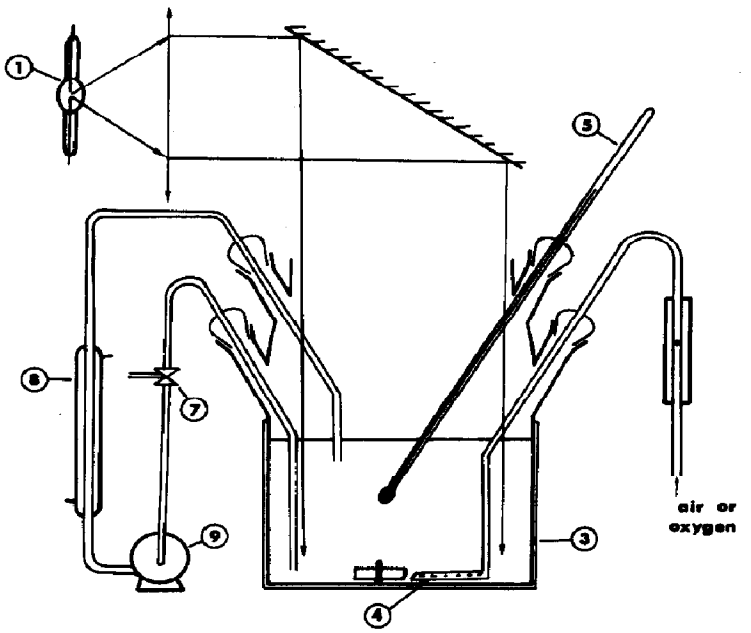


Fig. 3. Photoreactor with collimated light beam (solar simulator, mount B): 1, xenon lamp; all other numerals have same meaning as those in Fig. 2.

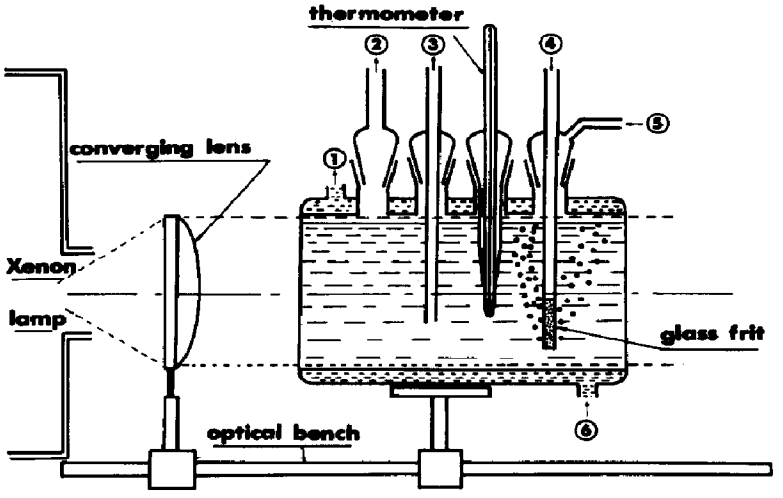


Fig. 4. Photoreactor with collimated light beam and gas collection (mount C): 1, 6, cooling-water ports; 2, gas exit to the gas chromatograph; 3, 5, recycled-solution ports; 4, gas inlet.

For E in the liquid

$$r_v = k_l a(C_{El} - C_{Ei}) + \frac{dC_{El}}{dt}$$

For E in the gas

$$k_l a(C_{El} - C_{Ei}) V_l = \bar{n}_{E\,out}$$

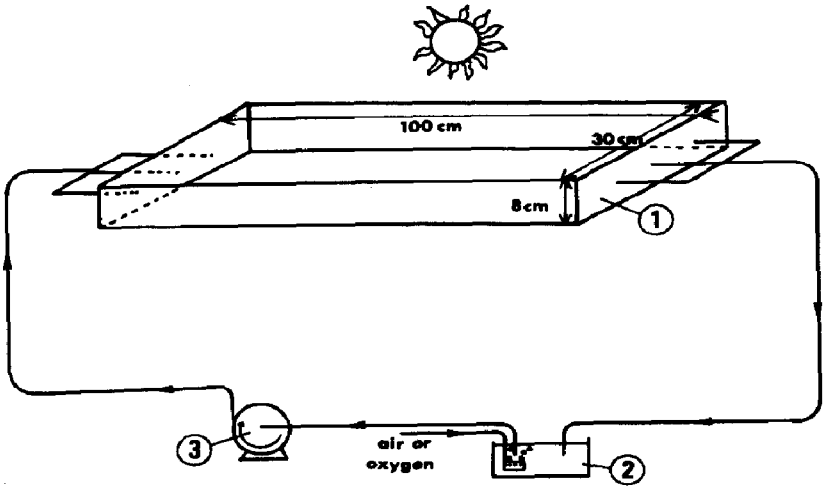


Fig. 5. Solar reactor (mount D): 1, reaction cell; 2, gas disperser; 3, recycling pump.

These equations can be simplified when the steady state is reached for D and E. Then

$$\frac{dC_{Dl}}{dt} = \frac{dC_{El}}{dt} = 0$$

$$r_v = \frac{\bar{n}_{D\,out}}{V_l} = \frac{\bar{n}_{E\,out}}{V_l}$$

Therefore, if $C_{Dl}$ and $C_{El}$ remain constant, so do $\bar{n}_{D\,out}$ and $\bar{n}_{E\,out}$, and they equal $r_v V_l$.

When a solid intervenes, as in the case of heterogeneous photocatalysis, liquid–solid interfacial transfer has to be taken into account, as reported earlier [5].

In photochemical reactors a further complication arises from the scattering of light. In Fig. 6, curve a shows the influence of an inert gas (nitrogen) on the rate of photodecomposition of oxalic acid (in mount B), and curve b shows the influence on the same reaction of a solid ($TiO_2$, rutile) known to be inert.

A rough model allows us to account for such curves (more elaborate models can be found in a recent review [6]). Let us assume, as in mount B, a parallel beam of light of intensity $I_0$ impinging on the solution. The intensity reflected from the inlet plane owing to the existence of the dispersed phase, *i.e.* of an interfacial area $a$ is

$$I_{ref} = \eta a I_0$$

The available intensity which penetrates the solution is therefore

$$I_l = I_0 - I_{ref}$$

In the case of bubbles, there is no absorption by the bubbles, and therefore $I_l$ is the photoactive intensity:

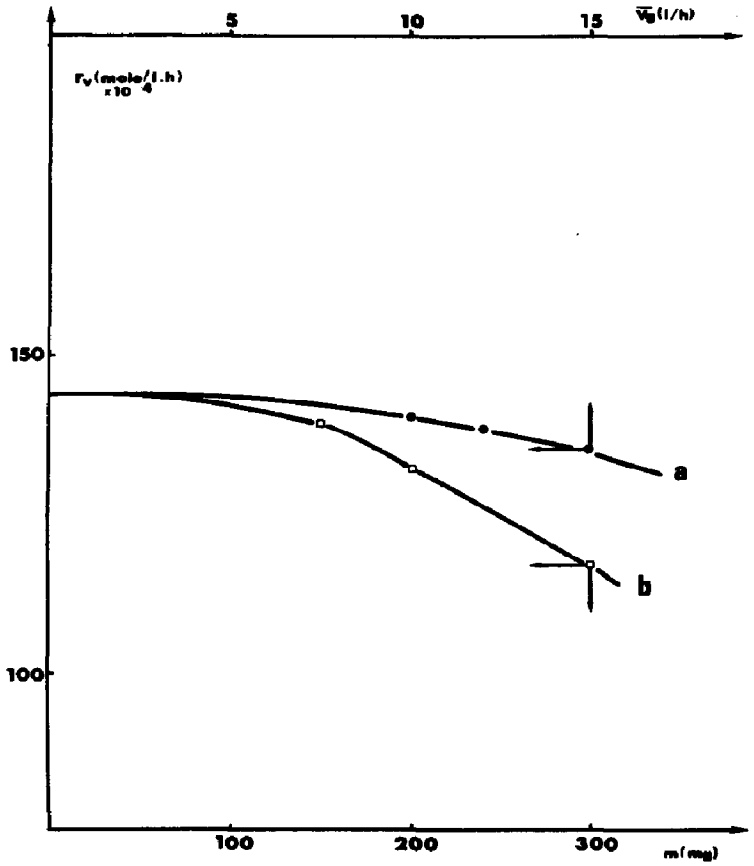


Fig. 6. Influence of an inert gas (curve a) and of an inert solid (curve b) on the photodecomposition of oxalic acid.

$$\frac{r_v}{r_{v_0}} = 1 - \frac{I_{ref}}{I_0} = 1 - \eta a$$

Let us assume that $a$ depends on the gas flow rate $\bar{V}_g$ (in the range of our measurements) [7] according to

$$a = A\bar{V}_g{}^m$$

Therefore

$$1 - \frac{r_v}{r_{v_0}} = B\bar{V}_g{}^m$$

Figure 7 shows that this relation is correctly obeyed with $m = 1$.

In the case of a solid dispersion, the absorption by the solid has to be taken into account, and this absorption varies with wavelength. Let us assume that in the case of $TiO_2$ this variation is from zero for $\lambda > 380$ nm to 100% for $\lambda < 380$ nm. In the former domain, as previously, we have

$$I_{photo} = I_0'(1 - a\eta)$$

where $I_0'$ is the incident intensity of wavelength longer than 380 nm.

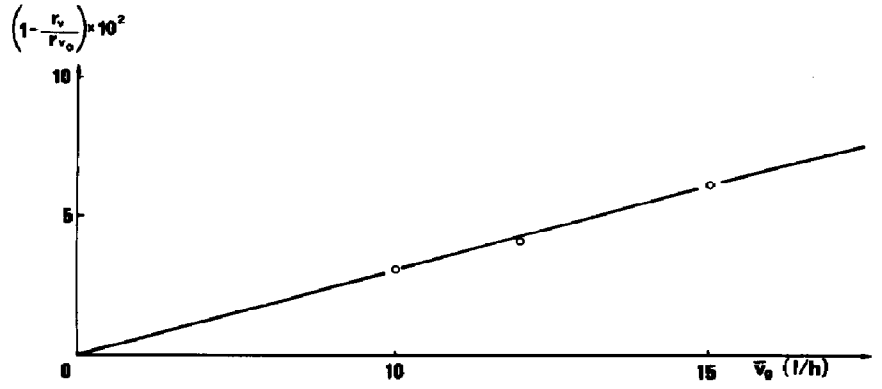


Fig. 7. Linear representation of curve a of Fig. 6.

In the latter domain, let us designate the napierian absorption coefficient of the species $k$ as $\mu_k$. If $i$ designates the photoactive species, then over a width $dx$ we have the following relation:

$$\frac{dI_{photo}}{dI_{abs}} = \frac{\mu_i C_i}{\alpha}$$

where $\alpha = \Sigma \mu_k C_k$. As there is no reflected intensity

$$I_{abs} = I_0''\{1 - \exp(-\alpha x)\}$$

where $I_0''$ is the incident intensity of wavelength shorter than 380 nm, then

$$dI_{abs} = I_0''\alpha \exp(-\alpha x)\, dx$$

$$dI_{photo} = I_0''\mu_i C_i \exp(-\alpha x)\, dx$$

$$I_{photo} = \frac{\mu_i C_i}{\alpha} I_0''\{1 - \exp(-\alpha x)\} \qquad (1)$$

Let us call $C_j$ the "concentration" of the absorbing solid. If the optical path $x$ is large enough, then

$$\frac{I_{photo}}{I_0''} = \frac{\mu_i C_i}{\mu_i C_i + \mu_j C_j}$$

If $\phi$, the overall quantum yield of the reaction, is supposed to be independent of the wavelength

$$r_v = \phi\left\{I_0'(1 - a\eta) + \frac{I_0''}{1 + (\mu_j C_j/\mu_i C_i)}\right\}$$

The many parameters involved in this formula prevent us from exploiting quantitatively curve b in Fig. 6.

## 3. Decarboxylation kinetics

### *3.1. Homogeneous medium*

The work devoted to the study of homogeneous (aqueous phase) decarboxylation of carboxylic acids is surprisingly rather scanty, if the special case of oxalic acid is excluded. Baur and Rebmann [8] reported the photosensitization of the decomposition of acetic acid with uranyl ions, and Heckler *et al.* [9] examined other organic acids (malonic, succinic and glutaric) more thoroughly. Interestingly, these researchers tried to relate the rate to the complexes formed between the uranyl ion and the organic acid, and we shall return to this point later.

We investigated the photodecarboxylation of acetic, propionic and butyric acids in the presence of various ions, *i.e.* $UO_2^{2+}$, $Fe^{3+}$ and the couple $Fe^{3+}$–$Cu^{2+}$. It is worth noting that whereas the uranyl ion concentration remains constant during the reaction the concentration of $Fe^{3+}$ decreases as $Fe^{2+}$ is formed. Therefore in these experiments $UO_2^{2+}$ appears to act as a catalyst and $Fe^{3+}$ as a reactant. Our results are summarized in Table 1. The striking feature is that, apart from the formation of $CO_2$ as a major product, the distribution of hydrocarbon products depends on the nature of the photoreceiver. This is especially manifest in the case of propionic acid and the $Fe^{3+}$–$Cu^{2+}$ couple, as shown in Fig. 8. There is also a marked difference in activity relative to $CO_2$ production in the photodecarboxylation of acetic acid under comparable conditions as exemplified in Fig. 9. Moreover, it is noteworthy that this production as a function of the cation to acid concentration ratio passes through a maximum. We shall return to this feature later.

The overall quantum yields of the studied decarboxylations have been determined from uranyl oxalate actinometry after a check on the

TABLE 1

**Observed photoproducts of the homogeneous photodecomposition of carboxylic acids**

| *Acid* | *Formula* | *Acid concentration* (mol $l^{-1}$) | *Photoreceiver range of concentration* (mol $l^{-1}$) | *Detected gaseous products* |
|---|---|---|---|---|
| Acetic acid | $CH_3COOH$ | $5 \times 10^{-2}$ | $5 \times 10^{-4} < [UO_2^{2+}] < 3 \times 10^{-2}$ | $CO_2 > CH_4 > C_2H_6$ |
| | | | $5 \times 10^{-4} < [Fe^{3+}] < 5 \times 10^{-2}$ | $CO_2 > C_2H_6 > CH_4$ |
| Propionic acid | $CH_3CH_2$-COOH | 1 | $10^{-2} < [Fe^{3+}] < 10^{-1}$ | $CO_2 > C_2H_6 > C_2H_4$ |
| | | | $[Fe^{3+}] = 10^{-2}$<br>$2.5 \times 10^{-6} < [Cu^{2+}] < 10^{-4}$ | $CO_2 > C_2H_4 > C_2H_6$ |
| Butanoic acid | $CH_3(CH_2)_2$-COOH | 1 | $[Fe^{3+}] = 10^{-2}$ | $CO_2 > C_3H_6$ ? > $C_3H_8$ ? |
| | | | $[Fe^{3+}] = 10^{-2}$<br>$[Cu^{2+}] = 10^{-2}$ | $CO_2 > C_3H_6$ |

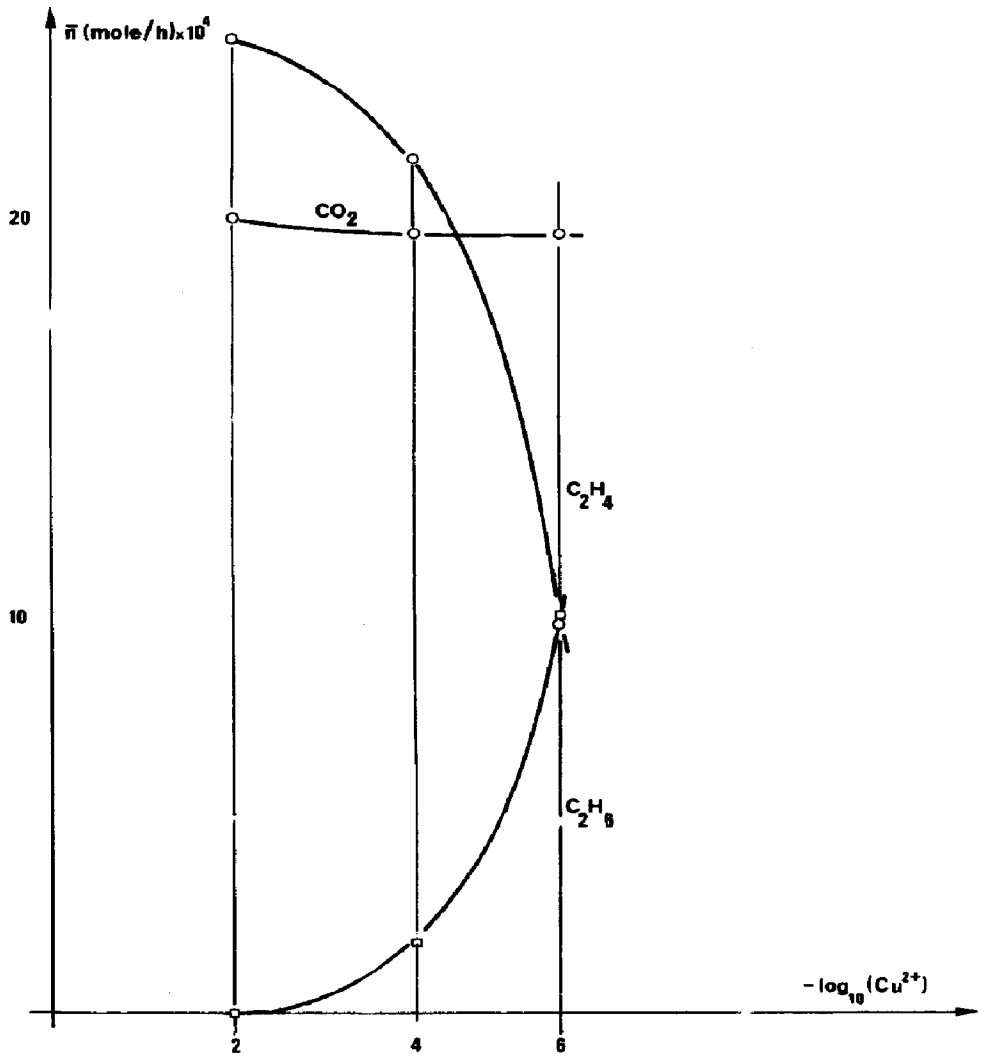


**Fig. 8. Effect of copper ion concentration on the gaseous products of propionic acid photodecomposition ([propionic acid] = 1 mol $l^{-1}$; [$Fe^{3+}$] = $10^{-2}$ mol $l^{-1}$).**

proportionality between the rate of $CO_2$ production and the absorbed intensity. Table 2 gives the results.

### *3.2. Heterogeneous systems*

Few studies have been concerned with the "photo-Kolbe" reaction at gas–solid interfaces. In a recent study [3], with gaseous acetic acid as a reactant and $TiO_2$ (platinized or not) as a catalyst, the following two reactions have been shown to occur:

$$CH_3CO_2H \longrightarrow CH_4 + CO_2$$

$$2CH_3CO_2H \longrightarrow C_2H_6 + 2CO_2 + H_2$$

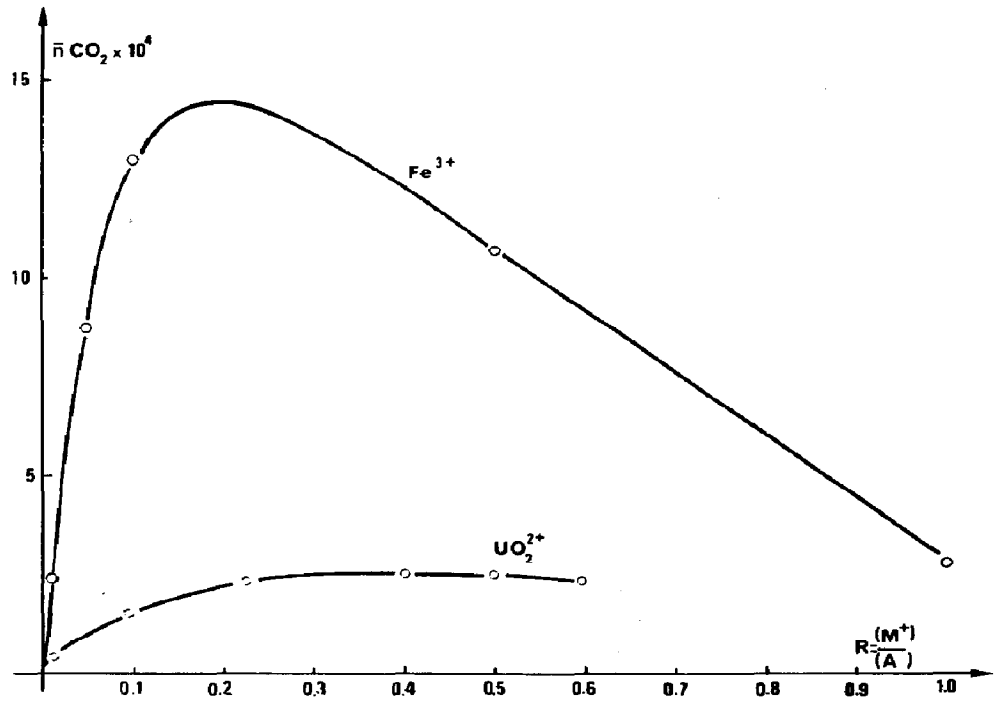


Fig. 9. Effect of the ratio $R = [M^+]/[A]$ on the $CO_2$ production in the photodecomposition of acetic acid ($[CH_3COOH] = 5 \times 10^{-2}$ M).

TABLE 2

Overall quantum yields of decarboxylation

| *Reactant* | *Photoreceiver* | $\phi$ (%)[a] |
|---|---|---|
| $CH_3COOH$ | $UO_2^{2+}$ | 0.4 |
| $CH_3COOH$ | $Fe^{3+}$ | 2 |
| $CH_3CH_2CO_2H$ | $Fe^{3+}$ | 11 |
| $CH_3(CH_2)_2CO_2H$ | $Fe^{3+}$ | 0.8 |

[a] $\phi$ = Moles of $CO_2$ produced (at maximum)/einsteins absorbed.

Both reactions are accelerated by the presence of water vapour, but the latter more than the former.

However, a number of studies deal with the decarboxylation of organic acids in aqueous solutions, and the main results are summarized in Table 3. An interesting observation in ref. 13 is the modification of the product distribution in the presence of $Ag^+$ ions which are strong electron acceptors.

## 4. Oxidation kinetics

### *4.1. Homogeneous catalysis*

There are surprisingly few examples in the literature of the homogeneous photocatalysis of the oxidation of carboxylic acids by oxygen. The

TABLE 3

Gaseous products of photodecomposition of carboxylic acids in the presence of heterogeneous catalysts

| *Carboxylic acid* | *Catalyst* | *Major products* | *Minor products* | *Reference* |
|---|---|---|---|---|
| Acetic acid | $TiO_2$ (anatase) $Pt/TiO_2$ | $CH_4$, $CO_2$ | $C_2H_6$, $H_2$ | 10 |
| Propionic acid | $Pt/TiO_2$ | $C_2H_6$, $CO_2$ | $C_2H_4$, $H_2$ | |
| Butanoic acid | $Pt/TiO_2$ | $C_3H_8$, $CO_2$ | $H_2$ | |
| Valeric acid | $Pt/TiO_2$ | $C_4H_{10}$, $CO_2$ | $H_2$ | |
| Pivalic acid | $Pt/TiO_2$ | Isobutane, $CO_2$ | Isobutene, $H_2$ | |
| Lactic acid | $Pt/TiO_2$ | $H_2$, $CO_2$, acetaldehyde | Ethanol, acetic acid, pyruvic acid | 11 |
| Lactic acid | Pt/CdS | $H_2$, pyruvic acid | | |
| Acetic acid | $Pt/TiO_2$ (rutile and anatase) | $CH_4$, $CO_2$, $H_2$ | $C_2H_6$, $H_2$, ethanol, acetaldehyde[a] | 12 |
| Acetic acid | $Pt/TiO_2$ (rutile and anatase) | $CH_4$, $CO_2$, $H_2$ | $C_2H_6$ | 13 |
| | | | Methanol, ethanol, acetone, propionic acid[a] | |
| Propionic acid | $Pt/TiO_2$ | $C_2H_6$, $CO_2$, $H_2$ | Ethanol, acetaldehyde, acetic acid, *n*-butanoic acid, pentanoic acid | |
| Levulinic acid | $Pt/TiO_2$ | $CO_2$, $CH_3COC_2H_5$, propionic acid, acetic acid | Methanol, ethanol, acetaldehyde, acetone, ethyl acetate, $CH_4$, $C_2H_6$ | 14 |

[a] Amounts depend on pH.

case of formic acid in the presence of $Fe^{3+}$ ions has been mentioned by Matsuura and Smith [15] and treated at length in our laboratory, initially with mount A [16]. Figure 10 shows the changes in the concentrations of formic acid, $Fe^{3+}$ and $Fe^{2+}$ as functions of time. The concentration $C_A$ of formic acid decreases monotonically to zero. Of course, $[Fe^{3+}] + [Fe^{2+}] = \text{const}$, so both concentrations vary oppositely. The "*macro*stationary" state is reached only at the end of the reaction. Detailed kinetic studies have shown that the rate $r_v$ of formic acid consumption per unit volume depends on the formic acid concentration $C_A$ according to

$$\frac{1}{r_v} = \frac{a}{C_A} + b$$

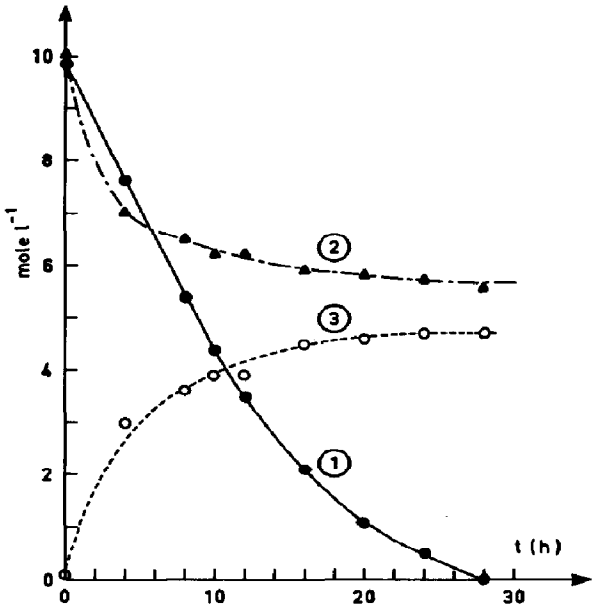


**Fig. 10. Variations in the concentrations of formic acid (curve 1), $Fe^{3+}$ (curve 2) and $Fe^{2+}$ (curve 3) with time in the photo-oxidation of formic acid: ●, $C_A$ (mol $l^{-1}$) × $10^2$; ○, [$Fe^{2+}$] (mol $l^{-1}$) × $10^4$; ▲, [$Fe^{3+}$] (mol $l^{-1}$) × $10^4$.**

In a batch reactor for A, the rate is

$$r_v = -\frac{dC_A}{dt}$$

so that the preceding relation can be integrated to give

$$a \ln C_A + bC_A = t_0 - t$$

It is noteworthy that such an expression accounts for the formic acid consumption with a solar simulator (mount B, Fig. 3) and with the sun itself (mount D, Fig. 5) (Fig. 11). Moreover, the rate $r_v$ is proportional to the absorbed light intensity, with an overall quantum yield $\phi$ found to be equal to 31% with mount A and 38% with mount B, which can be considered fair agreement.

The rate as a function of the concentration $C_{B1}$ of the dissolved oxygen is given by

$$\frac{1}{r_v'} = \frac{a'}{C_{B1}} + b'$$

Again, this expression has been confirmed independently with mount B.

The preceding equations can be checked more precisely under initial conditions:

For the reduction of $Fe^{3+}$ ions by formic acid

$$\frac{1}{r_{v_0\,red}} = \frac{\alpha}{C_{A_0}} + \frac{\beta}{C_t} + \gamma$$

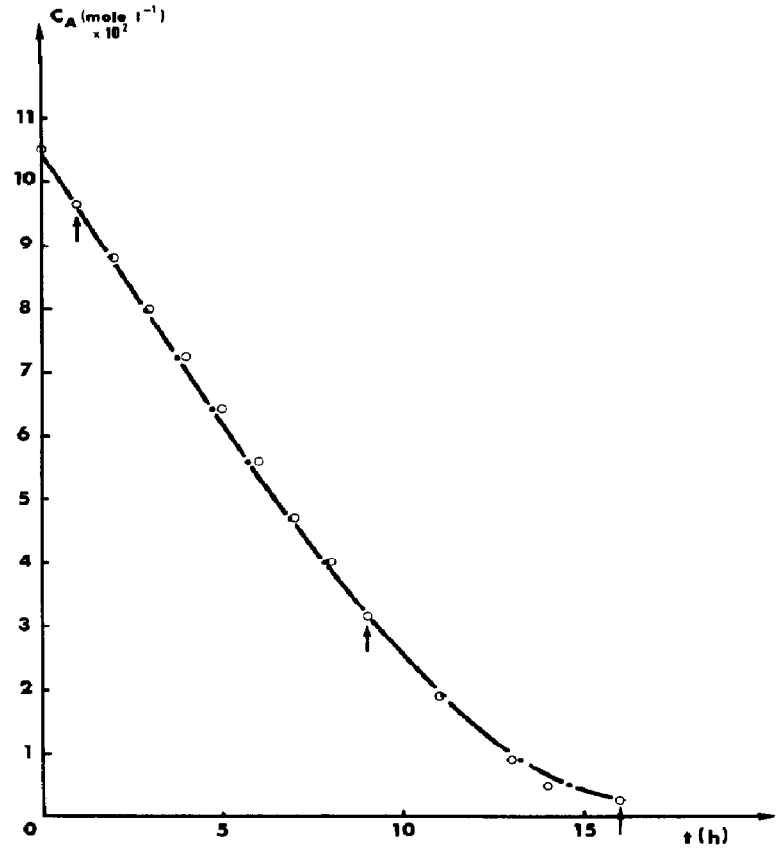


**Fig. 11. Formic acid consumption in the solar reactor. The full line corresponds to $a \ln C_A + bC_A = t_0 - t$ (the arrows indicate the values from which the constants $a$, $b$, $t_0$ have been calculated). The points are experimental measurements.**

where $C_t$ is the total concentration of iron (in the form of simple and complex ions).

For the oxidation of $Fe^{2+}$ ions by oxygen

$$\frac{1}{r_{v_0\,ox}} = \frac{\alpha'}{C_{A_0} C_{B10}} + \frac{\beta'}{C_{B10}} + \gamma'$$

Regardless of the detailed mechanism of each sequence, the overall reaction can be considered from now on as made up of two components: the first is the reduction of $Fe^{3+}$ by the carboxylic acid, and the second the oxidation of $Fe^{2+}$ by oxygen (Fig. 12). For each sequence the rates are respectively

$$r_{v\,red} = -\frac{1}{2}\left(\frac{d[Fe^{3+}]}{dt}\right)_I = \frac{1}{2}\left(\frac{d[Fe^{2+}]}{dt}\right)_I$$

$$r_{v\,ox} = \frac{1}{2}\left(\frac{d[Fe^{3+}]}{dt}\right)_{II} = -\frac{1}{2}\left(\frac{d[Fe^{2+}]}{dt}\right)_{II}$$

The *net* rates of variation in these concentrations are expressed by

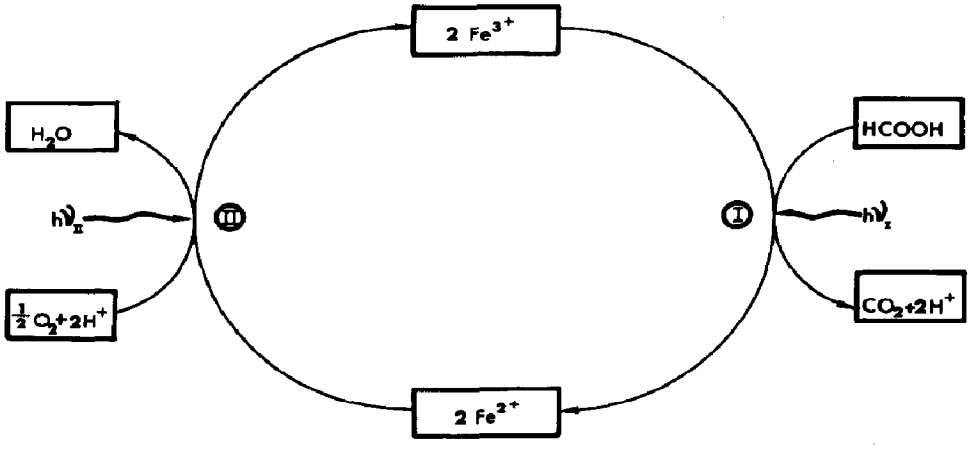


**Fig. 12. Overall mechanism of formic acid photo-oxidation by oxygen in the presence of iron ions.**

$$\left(\frac{d[Fe^{3+}]}{dt}\right)_{net} = 2(r_{v\,ox} - r_{v\,red}) = -\left(\frac{d[Fe^{2+}]}{dt}\right)_{net}$$

These equations, which derive from the stoichiometry, hold at any time. However, they do not imply that

$$\left(\frac{d[Fe^{3+}]}{dt}\right)_{net} = 0$$

as shown in our experiments (Fig. 10).

The extension of these findings to other carboxylic acids is not obvious. For instance, if we take a "standard" solution of 0.1 mol $l^{-1}$ of acid, $10^{-3}$ mol $l^{-1}$ of $Fe^{3+}$, and a "standard" gaseous flow of 1 l $h^{-1}$ of oxygen and 2 l $h^{-1}$ of carrier gas, we find the following rates for the oxidation: rate of oxidation of formic acid, $50 \times 10^{-4}$ mol $l^{-1}$ $h^{-1}$; rate of oxidation of acetic acid, $0.6 \times 10^{-4}$ mol $l^{-1}$ $h^{-1}$; rate of oxidation of oxalic acid, $39 \times 10^{-4}$ mol $l^{-1}$ $h^{-1}$.

This is why we "extended" the previous results only to oxalic acid (mount C). Our results are summarized in Fig. 13. The prolongation of the curves is limited by the precipitation of iron and copper oxalates. It is worth noting that they have been obtained starting from the nitrates of these ions. There is indeed a slight influence of the anions, the best results being obtained with the sulphates (a 20% increase). With a rate of $10.3 \times 10^{-3}$ mol $l^{-1}$ $h^{-1}$, the quantum yield is about 28%.

*4.2. Heterogeneous catalysis*

Few studies have been devoted to the oxidation of carboxylic acids by oxygen in aqueous solution [17], and the same is true of their anodic oxidation at an electrode [18, 19]. The recognized best photocatalyst is $TiO_2$ in the form of anatase, and Herrmann *et al.* [17] found that in the oxidation of

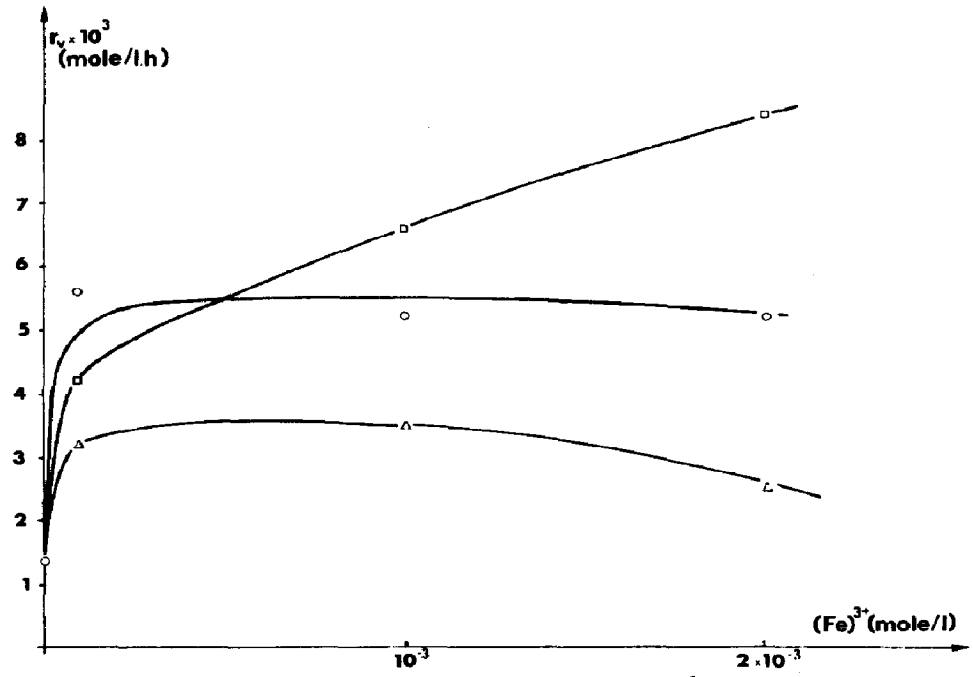


Fig. 13. Photo-oxidation of oxalic acid (0.1 mol $l^{-1}$) by oxygen in the presence of iron and copper ions: □, $[Cu^{2+}] = 10^{-3}$ mol $l^{-1}$; ○, $[Cu^{2+}] = 10^{-4}$ mol $l^{-1}$; △, $[Cu^{2+}] = 0$.

oxalic acid its activity can be related to a Langmuir-type isotherm for the adsorption of this reactant.

We also addressed ourselves to the use of $TiO_2$ in an earlier study of formic acid oxidation [5], and managed to increase significantly the rate of photocatalysis by using a *dissolved* substance which acts in synergy with anatase. With non-metallated phthalocyanine, we obtained the results shown in Fig. 14. Another drastic change is exemplified by $Cu^{2+}$ ions, as shown in Fig. 15. Depending on the anion which accompanies this cation, there is an increase in the rate which can be as high as 14-fold (the activity of $Cu^{2+}$ in the absence of $TiO_2$ is zero).

## 5. Discussion of experimental results: tentative mechanisms

### *5.1. Homogeneous medium*

The existence of a maximum in Fig. 9, strongly suggests that a complex must be formed between the photoreceiver and the reactant for the reaction to proceed. This assumption has already been made by Heckler *et al.* [9]. However, there is usually more than one such complex. For instance, in the case of uranyl ions in an aqueous solution of acetate $(AcO)^-$ ions the following components, among others, are well characterized: $UO_2^{2+}$, $UO_2(AcO)^+$, $UO_2(AcO)_2$, $UO_2(AcO)_3^-$, $UO_2(OH)^+$ and $UO_2(OH)_2$. Their stability constants are known [20] and their concentrations can be computed for a given

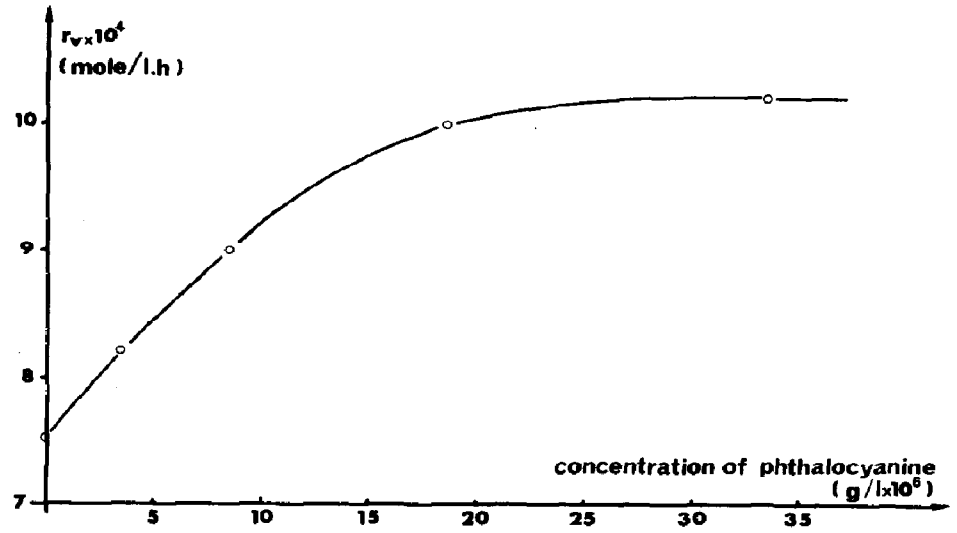


Fig. 14. Rate of formic acid photo-oxidation in the presence of $TiO_2$ (100 mg) and increasing amounts of phthalocyanine.

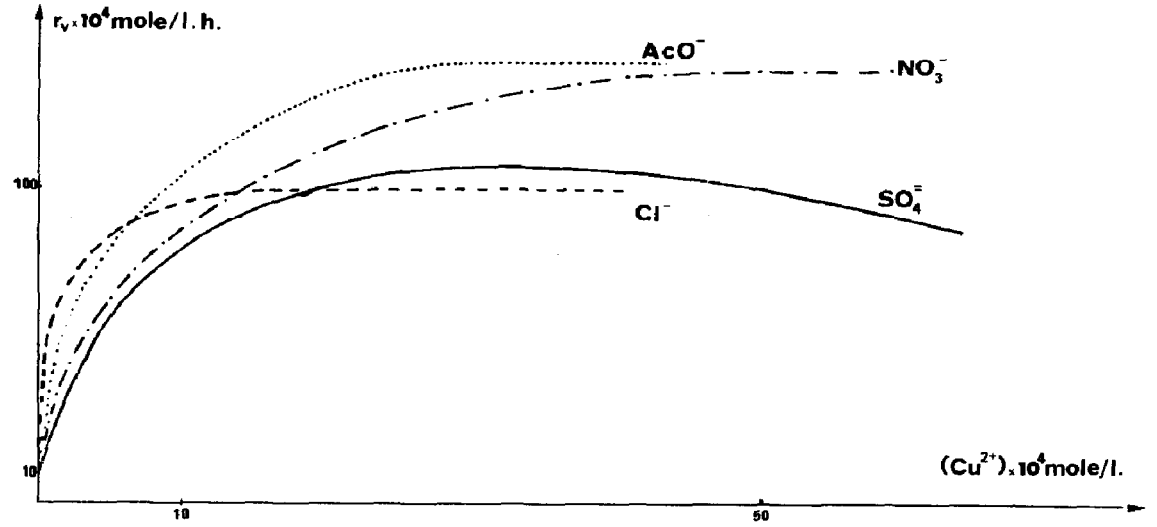


Fig. 15. Rate of photo-oxidation of formic acid (0.1 mol $l^{-1}$) in the presence of $TiO_2$ (100 mg) and increasing amounts of copper ions.

solution. Likewise, in the $Fe^{3+}$–formate ion system, besides free $Fe^{3+}$ ions, a number of absorbing complexes are known. These are, among others, $Fe(HCOO)^{2+}$ ($D_1$), $Fe(HCOO)_2^+$ ($D_2$), $Fe(HCOO)_3$ ($D_3$) and $Fe(HCOO)_4^-$ ($D_4$), to which the hydroxylated species $Fe(OH)^{2+}$ and $Fe(OH)_2^+$ may be added. When light is passed through a solution containing these species they all absorb, but we shall assume that only one of them is photoactive, *i.e.* that it undergoes the reaction. The same derivation as that leading to expression (1) gives

$$I_{photo} = \frac{\mu_i C_i}{\alpha} I_0$$

if the length $x$ is large enough. This expression can suffice to account for the kinetic findings in some instances. Two limiting cases may be considered.

(i) When the absorption coefficient of the complex $i$ is predominant, then $I_{photo}$ does not depend any longer on its concentration.

(ii) When the absorption coefficient of the complex $i$ is weak, then $I_{photo}$ is proportional to its concentration.

Let us consider again the oxidation of formic acid in the presence of iron, and assume, for the sake of simplicity, that the complex $Fe(HCOO)^{2+}$ ($D_1$) is the only *photoactive* species, and that it gives rise to the so-called Stern–Volmer sequence:

(1) $Fe^{3+} + HCOOH \rightleftharpoons Fe(HCOO)^{2+} + H^+$

(2) $Fe(HCOO)^{2+} \xrightarrow{h\nu} Fe(HCOO)^{2+*}$

(3) $Fe(HCOO)^{2+*} + HCOOH \longrightarrow$ deactivation

(4) $Fe(HCOO)^{2+*} + Fe^{3+} \longrightarrow$ deactivation

(5) $Fe(HCOO)^{2+*} + Fe(HCOO)^{2+} \longrightarrow$ deactivation

(6) $Fe(HCOO)^{2+*} \longrightarrow$ products

The last step is rate determining:

$$r = r_6 = k_6[D_1^*]$$

Assuming that the *micro*stationary state is reached for $D_1^*$, we have

$$I_{photo} = k_3[D_1^*][A] + k_4[D_1^*][Fe^{3+}] + k_5[D_1^*][D_1] + k_6[D_1^*]$$

Hence, in the case of weak absorbance

$$[D_1^*] = \frac{k_2[D_1]}{k_3[A] + k_4[Fe^{3+}] + k_5[D_1] + k_6}$$

From the equilibrium (1) it follows that

$$[D_1] = \frac{K_1[Fe^{3+}][A]}{[H^+]}$$

or, at a given pH

$$[D_1] = K_1'[Fe^{3+}][A]$$

Let us assume, by neglecting the concentrations of other complexes, that

$$C_t \simeq [Fe^{3+}] + [D_1]$$

$$[D_1] = \frac{K_1'[A]C_t}{1 + K_1'[A]} \qquad Fe^{3+} = \frac{C_t}{1 + K_1'[A]}$$

Therefore

$$\frac{1}{r} = \frac{1 + K_1'[A]}{k_6 k_2 K_1'[A] C_t}\left(k_3[A] + \frac{k_4 C_t}{1 + K_1'[A]} + \frac{k_5 K_1'[A] C_t}{1 + K_1'[A]} + k_6\right)$$

This expression is close to Yapi's experimental observations [16], provided $K_1'[A] < 1$. $K_1' = K_a K_1/[H^+]$, where $K_1$ is the stability constant of complex $D_1$ and is close to 31, according to ref. 21. $K_a$ is the acidity constant of formic acid (about $1.8 \times 10^{-4}$) and, as $H^+ \approx 5 \times 10^{-3}$ in our experiments, $K_1' \approx 1.1$. As $[A] = 10^{-1}$, $K_1'[A] \simeq 0.1$ which gives an order of magnitude of the error that we are introducing in neglecting it in comparison with unity. The knowledge of equilibrium constants allows us to calculate with a computer the proportions of the different formato complexes of iron as functions of pH. Figure 16 shows the curves obtained for $D_1$, $D_2$, $D_3$ and $D_4$. The first results obtained for the rate of photocatalysis are close to the curve for $D_1$, and therefore are in agreement with the mechanism proposed above.

However, this does not exclude the possibility of other mechanisms, which, for catalysis as a whole, should be consistent with a redox process (Fig. 12). The accelerating role of copper is worth discussing in relation to such a cycle. It seems [22] that copper intervenes in the reoxidation of $Fe^{2+}$

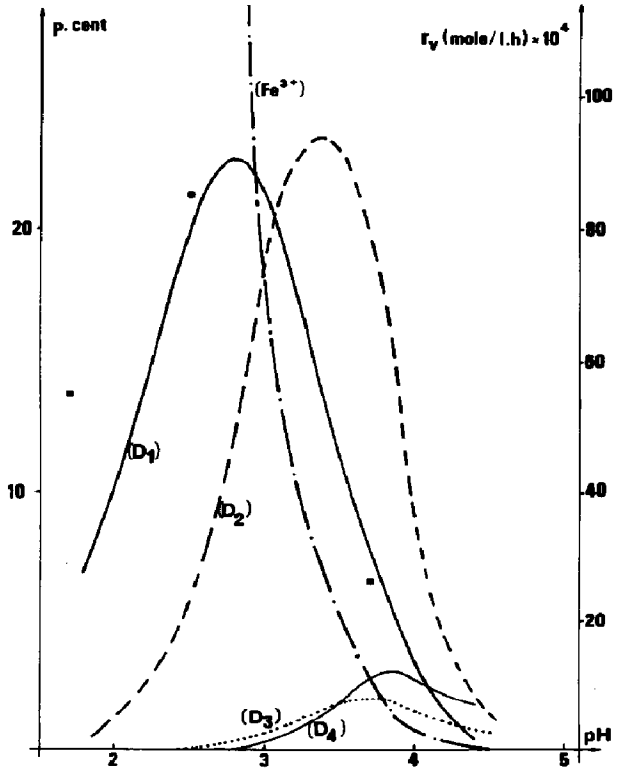


Fig. 16. Variations with pH in the proportions of the $Fe^{3+}$ concentration, and of the concentrations of the complexes $D_1$, $D_2$, $D_3$ and $D_4$ and in the rate of photo-oxidation of formic acid (■).

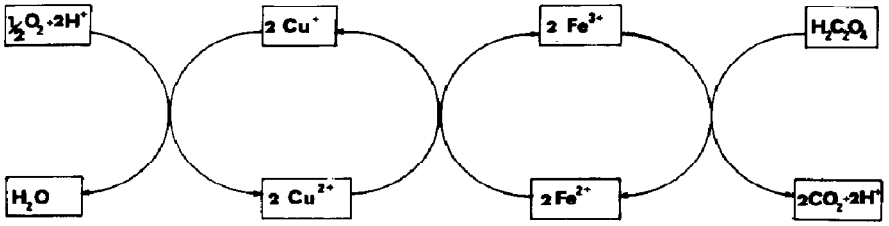


Fig. 17. Redox cycle of joint photocatalysis by iron and copper ions.

by introducing a cycle of its own, with the probable formation of $Cu^+$ ions, the formation of complexes adjusting the redox potentials to convenient levels (Fig. 17).

*5.2. Heterogeneous catalysis*

The present well-documented mechanism basically depends on the creation of an electron–hole pair with light of a convenient wavelength. The electron reduces the adsorbed electron acceptor species, and the hole oxidizes the adsorbed electron-donating species. What is less well known is the interpretation of the accelerating role of cations such as $Cu^{2+}$ on the oxidation of carboxylic acids in the presence of $TiO_2$. We tentatively propose the model shown in Fig. 18: the doping ions are adsorbed on the surface as specks on which the rate is different from the rate on the bare surface. It is logical to assume that the rate $r_{v_1}$ on the specks is proportional to the fraction $\theta$ of the surface covered, whereas the rate $r_{v_2}$ on the bare surface is proportional to $1 - \theta$. The global reaction rate $r_v$ is the sum $r_{v_1} + r_{v_2}$, and therefore

$$r_v = a\theta + b(1 - \theta) = (a - b)\theta + r_{v_0}$$

A result of these formal derivations is that the observed rate $r_v$ is proportional to $\theta$, which is itself a function of the concentration $C_M$ of the doping agent in the solution. This function is an adsorption–desorption isotherm, if it is assumed that the corresponding equilibrium is reached. Among the various forms of such isotherms, that of Langmuir has already been applied to $TiO_2$ in the presence of various solutes [17, 23]. With this hypothesis, we have

$$r_v - r_{v_0} = \frac{(a - b)KC_M}{1 + KC_M}$$

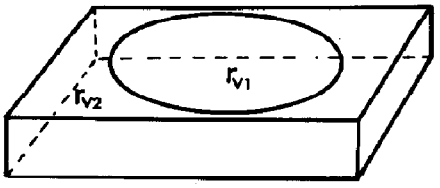


Fig. 18. "Leopard-skin" model for the interpretation of the accelerating role of $Cu^{2+}$ ions in the photo-oxidation of carboxylic acids in the presence of $TiO_2$.

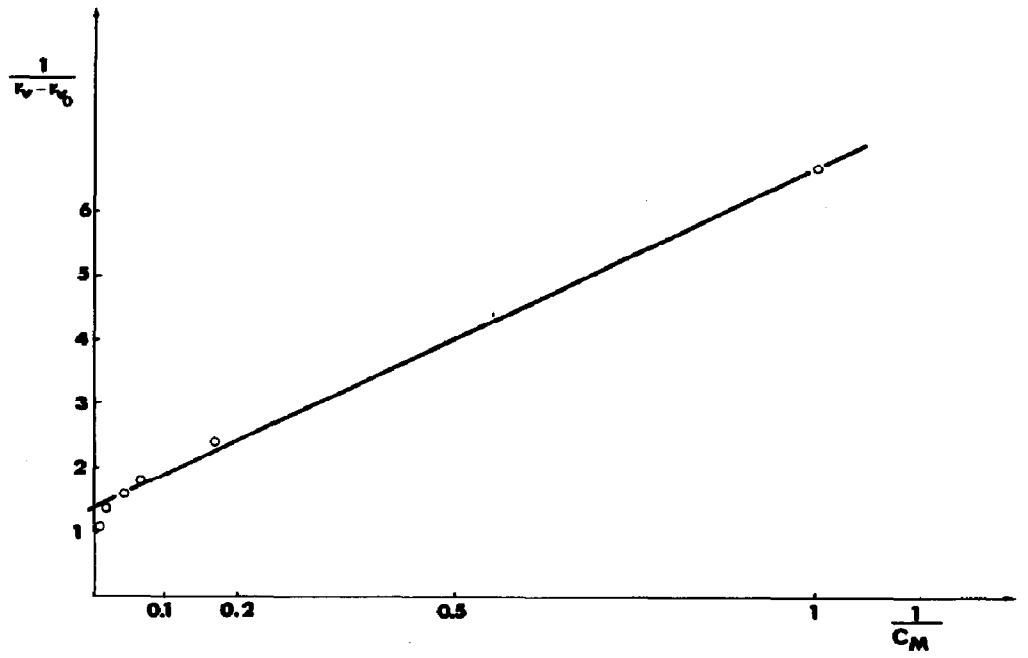


Fig. 19. Linear representation of the rate obtained in the presence of $TiO_2$ and $CuCl_2$ (Fig. 15).

and it must be checked that $1/(r_v - r_{v_0})$ is a linear function of $1/C_M$. Figure 19 shows that this check is fair.

It must be stressed again that these considerations are formal, and that they need direct substantiation by experimental evidence. A possible model could be a redox mechanism, analogous to that of Fig. 12, occurring on the specks at a rate greater than that in the mechanism on the bare surface. Another possibility is the adsorption of $Cu^{2+}$ ions on the TiOH surface groups, which could favour the adsorption of formate ions and possibly their transformation.

## 6. Conclusion

Photocatalytic systems, both for decarboxylation and for oxidation of carboxylic acids are numerous, but, with the possible exception of anatase and platinized anatase, no "universal" catalyst exists. An interesting domain to explore is the "tailoring" of catalysts, as indicated here, both with respect to their activity (as for ions in the presence of $TiO_2$) and to their selectivity (as for the couple $Fe^{3+}$–$Cu^{2+}$).

## Acknowledgments

The authors are indebted to the Centre National de la Recherche Scientifique (CNRS), Programme Interdisciplinaire de Recherches sur les Sciences

pour l'Energie et les matières premières (PIRSEM) for the grant received for the accomplishment of their research. They also wish to express their gratitude to Professor Dr. D. Rehorek from the Sektion Chimie der KMU in Leipzig (G.D.R.) and to Dr. Yapi from the University of Abidjan (Ivory Coast) for the part they took in this work.

## References

1 J. G. Calvert and J. N. Pitts, *Photochemistry*, Wiley, 1967, p. 429.
2 J. P. Utley, in N. L. Weinberg (ed.), *Techniques of Electro-organic Synthesis*, Part I, Wiley, New York, 1974, p. 793.
3 S. Sato, *J. Phys. Chem.*, *87* (1983) 3531.
4 B. Claudel, M. Bideau, L. Faure, J. P. Puaux, N. Taghizadeh, Z. Z. Yan and A. Yapi, *J. Photochem.*, *30* (1985) 25.
5 M. Bideau, B. Claudel and M. Otterbein, *J. Photochem.*, *14* (1980) 291.
6 O. M. Alfano, R. L. Romero and A. E. Cassano, *Chem. Eng. Sci.*, *41* (1986) 1137.
7 Y. T. Shah, B. G. Kelkar, S. P. Godbole and W. D. Deckwer, *AIChE J.*, *28* (1982) 353.
8 E. Baur and A. Rebmann, *Helv. Chim. Acta*, *5* (1922) 771.
9 G. E. Heckler, A. E. Taylor, C. Jensen, D. Percival, R. Jensen and P. Fung, *J. Phys. Chem.*, *67* (1963) 1.
10 B. Kraeutler and A. J. Bard, *J. Am. Chem. Soc.*, *100* (1978) 5985.
11 H. Harada, T. Sakata and T. Ueda, *J. Am. Chem. Soc.*, *107* (1985) 1773.
12 H. Yoneyama, Y. Takao, H. Tamura and A. J. Bard, *J. Phys. Chem.*, *87* (1983) 1417.
13 T. Sakata, T. Kawai and K. Hashimoto, *J. Phys. Chem.*, *88* (1984) 2344.
14 H. L. Chum, M. Ratcliff, F. L. Posey, J. A. Turner and A. J. Nozik, *J. Phys. Chem.*, *87* (1983) 3089.
15 T. Matsuura and J. M. Smith, *AIChE J.*, *16* (1970) 1064.
16 A. Yapi, *Doctoral Dissertation*, Lyon, 1984.
17 J. M. Herrmann, M. N. Mozzanega and P. Pichat, *J. Photochem.*, *22* (1983) 333.
18 K. Hirano and A. J. Bard, *J. Electrochem. Soc.*, *127* (1980) 1056.
19 K. Hirano, K. Inagaki, Y. Asami and R. Takagi, *Denki Kagaku*, *51* (1983) 893.
20 D. D. Perrin, *Stability Constants of Metal–Ion Complexes. Part B: Organic Ligands*, Pergamon, Oxford, 1977.
21 V. I. Paramonova, V. Y. Zamanskii and V. B. Kolychev, *Zh. Neorg. Khim.*, *17* (1972) 1042.
22 H. Tamura, K. Sato and M. Nagayama, *Nippon Kagaku Kaishi*, (1983) 1405.
23 D. F. Ollis, in E. Pelizzetti and N. Serpone (eds.), *Homogeneous and Heterogeneous Photocatalysis*, NATO ASI Series, Vol. 174, Reidel, Dordrecht, 1986, p. 651.

## Appendix A: Nomenclature

| | |
|---|---|
| *a* | interfacial area (or constant) |
| A | reactant |
| *A* | constant |
| B | reactant |
| *B* | constant |
| *C* | concentration |
| D | complex (or reaction product) |

| | |
|---|---|
| E | reaction product |
| $I$ | light intensity |
| $K$ | equilibrium constant |
| $k$ | rate constant, transfer coefficient |
| $n$ | number of moles |
| $r$ | reaction rate |
| $R$ | concentration ratio |
| $V$ | volume |
| $x$ | optical length |

*Greek letters*

| | |
|---|---|
| $\alpha$ | $\Sigma\mu_i C_i$ (or constant) |
| $\beta$ | constant |
| $\gamma$ | constant |
| $\eta$ | constant |
| $\theta$ | fraction of covered surface |
| $\mu$ | napierian absorption coefficient |
| $\rho$ | density |
| $\phi$ | overall quantum yield |

*Subscripts*

| | |
|---|---|
| A | pertaining to the component A |
| B | pertaining to the component B |
| D | pertaining to the component D |
| E | pertaining to the component E |
| g | in the gas phase |
| $i$ | pertaining to component $i$ (or at the interface) |
| l | in the liquid phase |
| net | net rate |
| ox | pertaining to oxidation |
| photo | photoactive intensity |
| red | pertaining to reduction |
| ref | reflected intensity |
| t | total |
| v | per unit volume |